



HAL
open science

Reactive ionized physical vapor deposition of thin films

S. Konstantinidis, R. Snyders

► **To cite this version:**

S. Konstantinidis, R. Snyders. Reactive ionized physical vapor deposition of thin films. European Physical Journal: Applied Physics, 2011, 56 (2), pp.24002. 10.1051/epjap/2011110199 . hal-00746206

HAL Id: hal-00746206

<https://hal.science/hal-00746206>

Submitted on 28 Oct 2012

HAL is a multi-disciplinary open access archive for the deposit and dissemination of scientific research documents, whether they are published or not. The documents may come from teaching and research institutions in France or abroad, or from public or private research centers.

L'archive ouverte pluridisciplinaire **HAL**, est destinée au dépôt et à la diffusion de documents scientifiques de niveau recherche, publiés ou non, émanant des établissements d'enseignement et de recherche français ou étrangers, des laboratoires publics ou privés.

Reactive Ionized Physical Vapor Deposition of thin films.

Stephanos Konstantinidis¹ and Rony Snyders^{1,2}

¹*Chimie des Interactions Plasma Surface, CIRMAP, Université de Mons, Place du Parc 20, 7000 Mons, Belgium.*

¹*Materia Nova Research Center, Avenue Copernic 1, 7000 Mons, Belgium.*

Author to whom correspondence should be addressed:

Email : stephanos.konstantinidis@umons.ac.be

Tel : +32 65 55 49 56

Fax: +32 65 55 49 41

Abstract.

In this article, the experimental results obtained in our laboratory for the last ten years and related to the reactive Ionized Physical Vapor Deposition (IPVD) processes are reviewed. Titanium oxide and titanium nitride thin films were chosen as case studies. The titanium-based thin films were synthesized from a pure titanium target sputtered in a mixture of argon and reactive gas (oxygen or nitrogen). Two IPVD processes were investigated namely i) reactive magnetron sputtering amplified by a superimposed secondary inductively coupled plasma and ii) reactive High-Power Impulse Magnetron Sputtering (HiPIMS). These researches were dedicated to the understanding of the plasma and plasma-surface interaction chemistries by using advanced plasma diagnostic techniques such as energy resolved mass spectroscopy, time-resolved emission and absorption spectroscopy. The relationships between the plasma chemistry and energetics and the properties of the thin films are emphasized.

1. Introduction.

The plasma – based Magnetron Sputtering (MS) technology is often employed in the research and development of functional thin films. However, despite the numerous advantages of the MS deposition process, in some aspects, it suffers from the lack of control regarding i) the trajectory and ii) the energy of the film forming species, i.e. the sputtered atoms or clusters. Hence, the growth of films on complex - shape substrates leads rather to non-conformal deposition which prevents or limits the usage of MS for e.g. the microelectronics industry. The energy input, which is a key parameter in the thin film growth process [1, 2], can be managed to some extent either by heating or by biasing the substrate or by unbalancing the magnetron magnetic field configuration **as reported i.e. in [3]. By unbalancing the magnetron field lines, electrons are allowed to escape the magnetic field trap. This way,**

electrons may drag plasma ions through ambipolar diffusion or induce ionizing collisions close to the substrate surface. As a consequence, ion bombardment of the growing film is increased. Nevertheless, heating the substrate might be technically difficult or simply unsuitable as for thermally sensitive materials. On the other hand, substrate biasing or ion bombardment during dc MS might lead to the incorporation of background gas atoms into the film during growth as bombarding ions are mostly Ar^+ . The incorporation of noble gas atoms is often detrimental to the mechanical, electrical, optical properties of the coatings [4-8]. Moreover, biasing an insulating substrate is often a difficult task, especially on industrial coaters.

A solution, developed in the 80's, was to ionize film forming species by using a secondary, dense, plasma superimposed to the magnetron plasma (see [9] and references therein). In the 90's, it was shown that the ionization rate of the sputtered particle could be achieved by applying high-power electrical pulses to the magnetron target [9, 10]. During High-Power Impulse Magnetron Sputtering (HiPIMS), the average power is kept to the conventional dcMS level by adjusting the duty cycle to values typically $< 1\%$. However, the peak power density reached during the HiPIMS experiment is typically two to three orders of magnitude larger than the power reached during conventional dcMS experiments (i.e. several kW/cm^2). Hence, during an IPVD deposition process, the metal atoms are ionized, the film forming species can be deposited in trenches [11] and their energy controlled through an appropriate biasing of the sample holder. In this article we summarized several years of research devoted to the understanding of the plasma chemistry and its relationship to the film properties. To illustrate these studies, we center our attention on the sputtering of a titanium target in a reactive atmosphere of argon mixed with either oxygen or nitrogen in order to synthesize titanium oxide (TiO_2) or titanium nitride (TiN) thin films, respectively. Controlling the properties of the films (e.g. microstructure, phase constitution, composition, and density) is of particular importance as they will determine the final usage of the coating. As an example, titanium oxide may be amorphous, or crystallized under the anatase or the rutile forms. Recently, Mráz *et al.* [12] demonstrated that the energy-per-deposited atom rules the phase formation of the reactively sputtered TiO_2 films, whatever the film is synthesized by a DC or a RF power magnetron discharge. Anatase is formed for low average energy per atom (< 540 eV/Ti) while the formation of the rutile polymorph needs a higher supply of energy (> 1000 eV/Ti). The anatase / rutile phase mixture is generated for an intermediate average energy per incoming atom. Anatase is used for photocatalytic purposes in order to degrade organic pollutants [13] while rutile has an increased refractive index as compared to anatase [14].

2. Experimental setups.

2.1. The amplified magnetron discharge

Three deposition chambers were used in our studies. In the case of vacuum chamber #1 (VC1), a 2-inch (5.1 cm) circular magnetron was used in order to generate the reactive magnetron sputtering discharge amplified by a superimposed secondary inductively coupled plasma (ICP). The cathode was DC powered. An induction coil was set between the titanium sputtering target and the substrate holder, 5 cm above the cathode. The 8-cm in diameter coil was powered by a 13.56 MHz RF generator in order to generate the dense secondary plasma. In this case, the RF power could be increased up to 200W. The chemistry of the glow discharge was analyzed by Energy resolved Mass Spectroscopy (EMS) in order to gain insight on the ion energy distribution function (IEDF) and on the ion population (by recording the mass spectrum). Residual Gas Analysis (RGA) measurements were also carried out in order to monitor the oxygen consumption rate with respect to the working parameters, e.g. the power supplied to the ICP. More details can be found in [15]. Another vacuum chamber (VC2) was used in order to carry out Langmuir probe (LP), EMS, time resolved Optical Emission (OES) and Atomic Absorption Spectroscopy (AAS) measurements

during non reactive and reactive amplified MS experiments as described in [16-20]. In this case, reactive MS experiments were performed in an Ar/N₂ gas mixture [16]. During these experiments, a 10-cm in diameter titanium target was employed. The RF supplied 12 cm-in diameter induction coil was located 4 cm above the circular target and 2 cm below the substrate holder. The RF power could be increased to 500 W. By using these two experimental arrangements, the ratio between the target and the coil size and power were comparable. A schematic description of the VC1 and the VC2 is presented on Fig. 1.

2.2. The HiPIMS discharge.

A home-made and patented HiPIMS [21, 22] power supply producing short (< 20 μs) high-power electrical pulses was used in VC2 for plasma diagnostic measurements [23, 24]. **Typical repetition frequencies lie in the range between hundreds of Hz up to several kHz.** Another vacuum chamber, VC3 (TSD 400CD by HEF, France), equipped with a 45 x 15 cm² rectangular titanium target was powered either by an ENI REPG 50 DC bipolar pulsed generator or by the HiPIMS power supply in order to synthesize titanium oxide thin films [25].

2.3. Thin film characterization methods.

Characterization methods were used in order to determine the thin film physico – chemical properties. Especially in the case of VC1, X-Ray Photoelectron Spectroscopy (XPS) data i.e. film chemical composition, were acquired *in situ* in order to avoid oxidizing the coating top most layer by venting the samples [15] and therefore to insure that the film chemistry could be correlated to the plasma chemistry. X-Ray Diffraction (XRD) measurements were carried out to determine the phase constitution of the coatings deposited in various working conditions, in particular during DC bipolar pulsed MS and HiPIMS. Scanning Electron Microscopy (SEM) micrographs were obtained for the films deposited in DC and HiPIMS in order to observe the film cross section morphology [22]. Mechanical profilometry was used to estimate the film thickness and X-Ray Fluorescence (XRF) measurements were carried out to estimate the amount of titanium atoms deposited on the substrate surface. Finally, the refractive index has been determined by using photospectrometry in the visible range (550 nm).

3. Experimental results

3.1. ICP amplified magnetron discharge.

Langmuir probe measurements were carried out in VC2. The measurements showed that the electron density increased as the power supplied to the RF coil was increased. These experiments were first performed in pure argon while the magnetron was not powered hence no titanium atoms are sputtered. Then the electron density as measured between the coil and the substrate holder was increased from $n_e = 2.5 \times 10^{10} \text{ cm}^{-3}$ to $n_e = 1.3 \times 10^{11} \text{ cm}^{-3}$ as the RF power was increased from 50 W to 500 W. A similar increase could be reported as the RF power is increased from 0 to 500 W for a given DC sputter power at the magnetron (100 W). These data (Fig. 2a and 2b), obtained at 5 or 30 mTorr, would suggest an increase of the ion concentration in the plasma close to the substrate holder. Also, it could be understood that the ICP is more efficient at 30 mTorr, as the electron density increase up to $\sim 10^{11} \text{ cm}^{-3}$. Nevertheless, using the Langmuir probe it was impossible to determine which kind of atom (Ar or Ti) was ionized in the plasma.

By using OES [26] and AAS [17, 20] the ionization rate of the sputtered titanium atoms in VC2, at the same distance from the magnetron target was determined. These measurements carried out with a 500 W magnetron power, 30 mTorr (3.9 Pa) argon pressure demonstrated that the ionization rate was close to 25 % in these conditions. Moreover it was found that the production of metastable titanium atoms as well as the increase of the global gas

temperature as the RF power was increased has to be taken into account. Data from other studies are in line with these results [27-29]. AAS measurements also showed that the absolute density of Ti atoms was decreased as the target was nitrided [18]. Moreover, AAS and mass spectrometry data are correlated in describing the evolution of the metallic species as the target surface evolves, with the nitrogen content, from the metallic to the poisoned regime. It confirms the validity of mass spectrometry to qualitatively follow titanium neutral density in reactive mode. With 500W power injected to the ICP and 500W on the magnetron target, a total pressure of 3.9 Pa, the density of Ti (n_{Ti}) decreases from $n_{Ti} \sim 1.6 \times 10^{10} \text{ cm}^{-3}$ to $n_{Ti} \sim 4 \times 10^9 \text{ cm}^{-3}$ while the Ti^+ peak intensity as, monitored by mass spectroscopy, evolves from $\sim 5 \times 10^7$ CPS (Counts Per Second) down to $\sim 1 \times 10^7$ CPS. Nevertheless, the two sets of data were not correlated in describing the evolution of Ti^+ and Ti as the total pressure was increased from 0.7 to 9.1 Pa. This discrepancy is induced by geometrical and particle transport considerations. AAS measurements are performed by averaging over the vacuum chamber diameter while the mass spectrometry measurements are strictly local measurements, on the side wall of the vacuum chamber.

In parallel to the increase of the ionization rate of the metal vapor, the dissociation rate of the reactive gas was also studied by using mass spectroscopy [15, 30]. The oxygen molecules are dissociated to a large extent in the plasma bulk and therefore the plasma chemical reactivity was enhanced as O radical are very likely to recombine with the neighboring surfaces to produce an oxidized compound. Using the amplified discharge, the fully oxidized thin film could be obtained for lower oxygen partial pressure. In the case of tin oxide (SnO_2) it was even possible to reach the SnO_2 stoichiometry while sputtering the target in the metallic regime hence allowing the deposition rate of the tin oxide to be increased by a factor of 6. In the case of Ti, the enhanced dissociation of the oxygen molecules do not play a so significant role on the chemical mechanisms of the titanium oxide films formation. Indeed, in that case, the heat of formation of the TiO_2 compound from Ti and molecular O_2 is already extremely large (924 kJ/mol) [31]. Therefore, O_2 doesn't need to be dissociated to facilitate its combination with the titanium film on the sample surface.

As titanium is sputtered in an Ar/ N_2 reactive atmosphere in VC2 [16] it is found that powering the ICP plasma (500W) has two effects on the metal-compound transition. First, the discharge voltage decreases, for a given nitrogen partial mass flow. Secondly, amount of nitrogen needed to reach the transition is increased. These two effects are explained by the increase of ionic flux impinging on the target as the ICP is powered. If the current on the cathode is increased because of the ionization of the plasma particles, the discharge voltage has to decrease for a fixed power to the cathode. The clean-poisoned transition is displaced for the same reason. The intensified bombardment of the target by ions drained from the plasma prevents the target surface modification.

Mass spectroscopy diagnostic data also showed that several effects could be observed on the Ion Energy Distribution Function (IEDF) during amplified magnetron sputtering experiments. Whatever the vacuum chamber used (VC1 or VC2) or the working conditions (the reactive gas used, the pressure, the power at the magnetron target), a dramatic increase of the plasma potential (V_p) was measured. This increase could be related to the increase of the electron temperature as the RF power is increased (see Fig. 2a and b). Using VC2, V_p increased up to +80V during reactive sputtering in Ar/ N_2 mixture [16] with respect to the ground potential. It is worth being noticed as, if the sample is grounded, the ions impinging on the sample surface will be accelerated by an inherent electric potential difference of 80V in the sheath. This increase of V_p can be minimized by adding a capacitor in the coil-ground connection [32]. However, The floating potential (V_f), as measured by Langmuir probes in an argon atmosphere in VC2, increases too and the $V_p - V_f$ potential difference that would set the ion kinetic energy in the case of a floating substrate typically stays within a 10 V range. The IEDF acquired in the same working conditions [16] also showed a low energy ($E < V_p$) shoulder for Ar^+ , N_2^+ , and N^+ . This shoulder was not observed for the Ti^+ ions. This observation could be related to the increased probability of charge exchange reactions ($X_{plasma}^+ + X_{sheath} \rightarrow X_{plasma} + X_{sheath}^+$) in the RF sheath surrounding the mass spectrometer orifice. RF sheaths are typically wider than DC sheath [33] and if both the plasma ion population ($X_{plasma}^+ = Ar^+, N_2^+, \text{ or } N^+$) and the populations of the

corresponding neutral atoms/molecules (X) are large, symmetric charge exchange reaction are likely to occur. N₂ and Ar are the background gases. At a pressure of ~ 1 Pa, with a gas temperature of 300 K, the density is approximately of the order of 10¹³ cm⁻³ although the concentration of sputtered Ti is of the order of 10¹⁰ – 10¹¹ cm⁻³ depending on the power applied to the sputtering target [17, 20]. As a consequence, the probability of collision between Ti⁺ and Ti in the sheath is small and the cross section for asymmetric charge exchange between Ar and Ti is small. Due to the charge exchange reaction, the accelerated ion entering the sheath (X⁺_{plasma}) will exchange its positive charge with the neutral atom/molecule (at rest) in the sheath. The newly generated ion is accelerated by the sheath electric field. However it will only gain a fraction of the full kinetic energy that could be provided by the sheath electric field. Han *et al* [34], also investigated the influence of the ICP on the phase constitution of the TiO₂ film deposited. When the ICP (400 W) was amplifying the magnetron DC discharge (300 W), rutile – anatase phase mixture were observed on the non-intentionally heated samples. When only the DCMS discharge was used, the film was amorphous. It is assumed that enhanced ion diffusivity on the surface and ion bombardment play a significant role during thin film growth when the secondary plasma is present. More recently, Li *et al* [35] also showed that it was possible to synthesize high-quality anatase coatings on unheated substrate using an amplified magnetron. As for the comparison, Martin *et al* [14] studied the influence of post deposition annealing on amorphous titanium oxide films. Anatase films were produced by annealing to 300°C while rutile appeared next to the anatase diffraction peaks at a temperature of 700°C. Phase pure rutile was obtained at 900°C.

3.2. The HiPIMS discharge

Time resolved OES measurements were carried out during a HiPIMS discharge, in an oxygen/argon mixture (1 Pa) containing 50% of oxygen hence running the discharge in the oxidized regime. The VC2 was used and the pulse characteristics were: pulse voltage = 900 V, pulse duration = 10 μs. the discharge voltage started at 17 μs (the voltage rise time is ~0.1 μs) and stopped at 27 μs (decrease time is also ~0.1 μs). On Fig. 3, the evolution of the emission line intensities as a function of time are reported for Ti (363.5 nm), Ti⁺ (368.5 nm), O₂⁺ (602.4 nm), O (777.7 nm), and Ar (750.4 nm). The Ar and O₂⁺ line intensities showed a maximum. The Ti neutral line saturated at the end of the pulse, the Ti⁺ line intensity however increased until the end of the pulse i.e. as far as energy is supplied to the plasma. This behavior would highlight, if the line intensity can be related to the emitter ground state density, that i) an increase of the sputtered material ionization as the Ti⁺/Ti line intensity ratio increases ii) the increased dissociation rate of the molecular oxygen as the pulse evolves. This behavior is suggested by the increased O line intensity although the intensity of the O₂⁺ line showed a maximum after a few μs. As it can be seen on Fig. 3, the O₂⁺ actually vanished rapidly after the pulse started. The O/O₂⁺ line intensity ratio was also measured for a DC discharge in the same working conditions and the same average power supplied to the magnetron cathode. O/O₂⁺ line intensity ratio was increased 10 times in the case of the HiPIMS glow discharge. As for the RF amplified magnetron discharge, the increased electron density during the HiPIMS discharge allows for a strong ionization and dissociation of the molecular gas hence significantly increasing the ion bombardment during film growth as well as enhancing the plasma reactivity. The mass spectrum presented on Fig. 4 and recorded in the same working condition (oxidized target, HiPIMS discharge) would corroborate the time-resolved OES data. The O⁺-related line is intense (and even saturates). It should be also noted that TiO⁺ as well as TiO₂⁺ ionized molecules are present. A third feature regarding the time evolution of the argon line during the pulse could be remarked. Indeed, the argon line passes through a maximum. This would evidence gas rarefaction during the high-current pulse. The peak discharge current density in a HiPIMS discharge is typically two to three orders of magnitude larger than during a DC discharge, in the same working conditions and average power. Hence it can be expected that such an intense bombardment of the titanium target would increase the number of sputtered titanium atoms. Then the fast Ti atoms (the average kinetic energies are typically in the order of a few eV for magnetron sputtering [36]) would exchange their momentum with the argon background, provoking heating of the argon atmosphere and

therefore inducing a decrease of the argon density in the neighborhood of the sputtering target. This situation would be apparently achieved already after a few μs (See Intensity of the Ar line on Fig. 3). If the pulse lasts longer ($> 10 - 20 \mu\text{s}$), the sputtered metal ions are taking over the target surface sputtering, i.e. self-sputtering is triggered. As for Ti^+ , the self-sputtering yield is lower than the one of Ar^+ and as it is necessary to taking into account the increased involvement of the Ti^+ ions in the sputtering process and conversely their reduced contribution to the deposition procedure, it can be understood that the deposition rate is usually lower for longer high-power pulses, as described in [24]. This decrease of the film forming species flux at the substrate and the fact that they are ionized (see [37]) might stimulate dramatic changes in the film growth process hence leading to a modification of the film properties such as phase constitution, density, ...

Titanium oxide thin films were synthesized by using $7 \mu\text{s}$ long high-power pulses in the VC3. The target voltage was set to 900 V, the peak current reached with 50 % of oxygen in the reactive atmosphere was approximately 200 A. The time-averaged power on the target was set to 1.5 kW. Titanium oxide films were deposited by using a DC bipolar power supply as a reference. As reported in [25], the HiPIMS process leads to a modification of the film phase constitution especially if the films are deposited on a grounded surface e.g. a steel foil. In this case, the films exhibited a diffraction pattern corresponding to pure rutile. To the contrary, the DCMS films were containing only anatase nanocrystals. Concerning the film grown on glass, hence on a floating substrate, both deposition processes were leading to the formation of pure anatase. However, the diffraction pattern corresponding to the anatase film deposited by HiPIMS revealed a multi-oriented structure. It is suggested that keeping the substrate floating, e.g. by using a glass substrate, would lead to a modification of the electron and ion interactions with the substrate surface hence decreasing the effectiveness of the ion bombardment in such circumstances [25]. The refractive indices of the two anatase films deposited on glass were measured at 550 nm. They were 2.4 and 2.1 for the films synthesized by HiPIMS and by DCMS, respectively. This result would emphasize the increased film density as HiPIMS is employed. Similar results were obtained in the case of zinc oxide [38]. It was found that the film thickness was lower in the case of HiPIMS but the amount of deposited material, as determined by X-Ray Fluorescence was almost identical for both HiPIMS and DCMS films hence highlighting the improved packing density as HiPIMS is used. This report emphasizes the need to continue on carefully studying the mechanism of target poisoning during reactive HiPIMS.

Recent results [39], obtained on a 20 cm-long cylindrical rotating magnetron titanium target showed that during an HiPIMS deposition process, the amount of energy supplied per deposited atom is larger in the case of HiPIMS, as compared to the DCMS experiments performed in an identical environment, at the same average power. Calorimetric probe [40] measurements showed that the amount of energy supplied to the sample surface could be increased by using larger high-power pulses. As the deposition rate (i.e. the flux of depositing particles) was found to decrease as the pulse is lasting longer, it could be assumed that the energy flux increase was a consequence of the increased ionization rate of the metallic vapor, as the pulse was enlarged [24]. The amount of energy supplied per Ti atom increased from $\sim 2.5 \times 10^{-14}$ mWs for the DC discharge, to $\sim 5 \times 10^{-14}$ mWs (HiPIMS $5 \mu\text{s}$ long pulse) and to $\sim 10^{-13}$ mWs (HiPIMS with 15 or $20 \mu\text{s}$ pulses). Mass spectrometry measurements showed that in a HiPIMS discharge, the averaged ion energy is increased as compared to the corresponding DCMS discharge, as it was emphasized in the case of a titanium target sputtered in a Ar/N_2 atmosphere [41]. In the case of a Ar/O_2 gas mixture, energy could be supplied to the growing by O^- ions, leaving the target with a kinetic energy equal to the sheath potential (i.e. several hundreds of eV) [42, 43]. However, the presence of these fast heavy particles is not mandatory to the formation of the rutile structure in the case of HiPIMS discharges. In their experiments, Alami *et al* [44] demonstrated by tilting the substrate by 90° from the target plane that rutile films could be obtained without O^- bombardment. In these circumstances the film surface is solely bombarded by low energy ions (Ti^+ and Ar^+). Indeed, in HiPIMS discharges a large fraction of ion target current could be detected in a direction tangential to the magnetic field [45]. On the other hand, while studying the phase formation of hafnium oxide and oxynitride films synthesized by HiPIMS and

by DCMS, Sarakinos et al [46] highlighted the influence of the film and plasma chemistries on the film structure. By suppressing the O^- bombardment and by working in the transition zone (by using the HiPIMS power supply), they revealed that the incorporation of vacancies in the material could lead to the formation of the high-temperature cubic HfO_2 phase at room temperature.

4. Summary

In this article we have summarized several years of research dedicated to the understanding of two ionized physical deposition processes namely the magnetron discharge amplified by a secondary Inductively Coupled Plasma (ICP) and the High-Power Impulse Magnetron Sputtering (HiPIMS). The results reported here are mainly related to the reactive deposition process, when oxygen or nitrogen is added to the argon background gas in order to synthesize e.g. titanium oxide or titanium nitride thin films. Irrespective of the method used (ICP or High-power pulses) it was observed that increasing the power to the ICP plasma or increasing the pulse duration (i.e. the plasma burning time) leads to an increase of the electron density which in turn allows i) ionization rate of the sputtered metal and ii) dissociation rate of the reactive gas molecules to be increased. Increasing the ion flux to the substrate usually leads to an increase of the energy supply per deposited atom. This induces the formation of films with varied properties. With HiPIMS, films are found to be denser and the X-Ray diffraction patterns reveal a modified structure, e.g. the presence of high-temperature rutile phase or an anatase structure with multi-oriented nanocrystals. As a result, the refractive index of the transparent titanium oxide coating is dramatically increased. However, although ion bombardment is of tremendous importance for the film formation, materials and plasma-surface chemistry are also key parameters and it was shown that the HiPIMS discharge might also play a role in this case too.

5. Acknowledgements

The authors would like to thank the financial supports of the Belgian Government to the IAP program (P06/08) and of the Walloon Region (DGO6) through the Opti2mat program.

S. Konstantinidis thanks the National Fund for Scientific Research (FNRS, Belgium).

6. Bibliographic references

- [1] I. Petrov, F. Adibi, J.E. Greene, L. Hultman, J.E. Sundgren, *Appl. Phys. Lett.* 63/1 (1993) 36.
- [2] I. Petrov, P.B. Barna, L. Hultman, J.E. Greene, *J. Vac. Sci. Technol. A* 21/5 (2003) S117.
- [3] P.J. Kelly, R.D. Arnell, *Vacuum* 56/3 (2000) 159.
- [4] P. Catania, R.A. Roy, J.J. Cuomo, *J. Appl. Phys.* 74/2 (1993) 1008.
- [5] E. Mounier, Y. Pauleau, *Diamond and Related Materials* 6/9 (1997) 1182.
- [6] H. Windischmann, *Crit. Rev. Solid State Mat. Sci.* 17/6 (1992) 547.
- [7] J. Houska, O. Warschkow, M.M.M. Bilek, D.R. McKenzie, J. Vlcek, S. Potocky, *J. Phys.-Condes. Matter* 18/7 (2006) 2337.
- [8] H. Oettel, R. Wiedemann, S. Preissler, *Surf. Coat. Technol.* 74-5/1-3 (1995) 273.
- [9] U. Helmersson, M. Lattemann, J. Bohlmark, A.P. Ehasarian, J.T. Gudmundsson, *Thin Solid Films* 513 (2006) 1.
- [10] K. Sarakinos, J. Alami, S. Konstantinidis, *Surf. Coat. Technol.* 204 (2010) 1661.
- [11] J. Alami, P. Eklund, J.M. Andersson, M. Lattemann, E. Wallin, J. Bohlmark, P. Persson, U. Helmersson, *Thin Solid Films* 515 (2007) 3434.
- [12] S. Mraz, J.M. Schneider, *J. Appl. Phys.* 109/2 (2011).
- [13] A. Mills, S. LeHunte, *J. Photochem. Photobiol. A-Chem.* 108/1 (1997) 1.
- [14] N. Martin, C. Rousselot, D. Rondot, F. Palmino, R. Mercier, *Thin Solid Films* 300/1-2 (1997) 113.
- [15] R. Snyders, J.P. Dauchot, M. Hecq, *Plasma Processes and Polymers* 4/2 (2007) 113.
- [16] S. Konstantinidis, C. Nouvellon, J.P. Dauchot, M. Wautelet, M. Hecq, *Surface & Coatings Technology* 174 (2003) 100.
- [17] S. Konstantinidis, A. Ricard, M. Ganciu, J.P. Dauchot, C. Ranea, M. Hecq, *Journal of Applied Physics* 95/5 (2004) 2900.
- [18] S. Konstantinidis, A. Ricard, R. Snyders, H. Vandeparre, J.P. Dauchot, M. Hecq, *Surface & Coatings Technology* 200/1-4 (2005) 841.
- [19] C. Nouvellon, S. Konstantinidis, J.P. Dauchot, M. Wautelet, P.Y. Jouan, A. Ricard, M. Hecq, *Journal of Applied Physics* 92/1 (2002) 32.
- [20] A. Ricard, C. Nouvellon, S. Konstantinidis, J.P. Dauchot, M. Wautelet, M. Hecq, *Journal of Vacuum Science & Technology a-Vacuum Surfaces and Films* 20/4 (2002) 1488.
- [21] M. Ganciu, S. Konstantinidis, Y. Paint, J.P. Dauchot, M. Hecq, L. de Poucques, P. Vasina, M. Mesko, J.-C. Imbert, J. Bretagne, M. Touzeau, *J. Opt. Adv. Mat.* 7 (2005) 2512.
- [22] M. Ganciu, M. Hecq, J.P. Dauchot, S. Konstantinidis, J. Bretagne, L. de Poucques, M. Touzeau, *World Patent* 2004.
- [23] S. Konstantinidis, J.P. Dauchot, M. Ganciu, M. Hecq, *Applied Physics Letters* 88/2 (2006).
- [24] S. Konstantinidis, J.P. Dauchot, M. Ganciu, A. Ricard, M. Hecq, *Journal of Applied Physics* 99/1 (2006).
- [25] S. Konstantinidis, J.P. Dauchot, M. Hecq, *Thin Solid Films* 515/3 (2006) 1182.
- [26] C. Nouvellon, S. Konstantinidis, J.P. Dauchot, M. Hecq, *Vide-Science Technique Et Applications* 57/304 (2002) 243.
- [27] Y. Andrew, I. Abraham, J.H. Booske, Z.C. Lu, A.E. Wendt, *Journal of Applied Physics* 88/6 (2000) 3208.
- [28] L. de Poucques, J.C. Imbert, P. Vasina, C. Boisse-Laporte, L. Teule-Gay, J. Bretagne, M. Touzeau, *Surface & Coatings Technology* 200/1-4 (2005) 800.
- [29] L. Xu, N. Sadeghi, V.M. Donnelly, D.J. Economou, *Journal of Applied Physics* 101/1 (2007).
- [30] R. Snyders, R. Gouttebaron, J.P. Dauchot, M. Hecq, *Surf. Coat. Technol.* 200/1-4 (2005) 448.
- [31] 87th *Handbook of Chemistry and Physics*, CRC Press, Boca Raton (FL), 2006-2007.
- [32] J.N. Kim, H.Y. Lee, D.K. Lee, J.J. Lee, *Surf. Coat. Technol.* 201/9-11 (2007) 5442.
- [33] M. Zeuner, H. Neumann, J. Meichsner, *J. Appl. Phys.* 81/7 (1997) 2985.
- [34] Y.H. Han, S.J. Jung, J.J. Lee, *Surf. Coat. Technol.* 201/9-11 (2007) 5387.
- [35] Z.G. Li, S. Miyake, *Acta Metall. Sin.* 46/1 (2010) 13.
- [36] B. Chapman, *Glow Discharge Processes*, John Wiley & Sons 1981.
- [37] A.P. Ehasarian, A. Vetushka, A. Hecimovic, S. Konstantinidis, *J. Appl. Phys.* 104 (2008) 83305.
- [38] S. Konstantinidis, A. Hemberg, J.P. Dauchot, M. Hecq, *J. Vac. Sci. Technol. B* 25 (2007) L19.

- [39] W. Leroy, S. Konstantinidis, S. Mahieu, R. Snyders, D. Depla, *J. Phys. D: Appl. Phys.* 44 (2011).
- [40] H. Kersten, H. Deutsch, H. Steffen, G.M.W. Kroesen, R. Hippler, *Vacuum* 63/3 (2001) 385.
- [41] A.P. Ehasarian, Y.A. Gonzalvo, T.D. Whitmore, *Plasma Process and Polymers* 4 (2007) S309.
- [42] S. Mraz, J.M. Schneider, *Applied Physics Letters* 89/5 (2006).
- [43] S. Mraz, J.M. Schneider, *J. Appl. Phys.* 100/2 (2006).
- [44] J. Alami, K. Sarakinos, F. Uslu, C. Klever, J. Dukwen, M. Wuttig, *J Phys D Appl Phys* 42/11 (2009).
- [45] D. Lundin, P. Larsson, E. Wallin, M. Lattemann, N. Brenning, U. Helmersson, *Plasma Sources Sci. Technol.* 17 (2008) 035021.
- [46] K. Sarakinos, D. Music, S. Mraz, M.T. Baben, K. Jiang, F. Nahif, A. Braun, C. Zilkens, S. Konstantinidis, F. Renaux, D. Cossement, F. Munnik, J.M. Schneider, *Journal of Applied Physics* 108/1 (2010).

6. Figures and captions

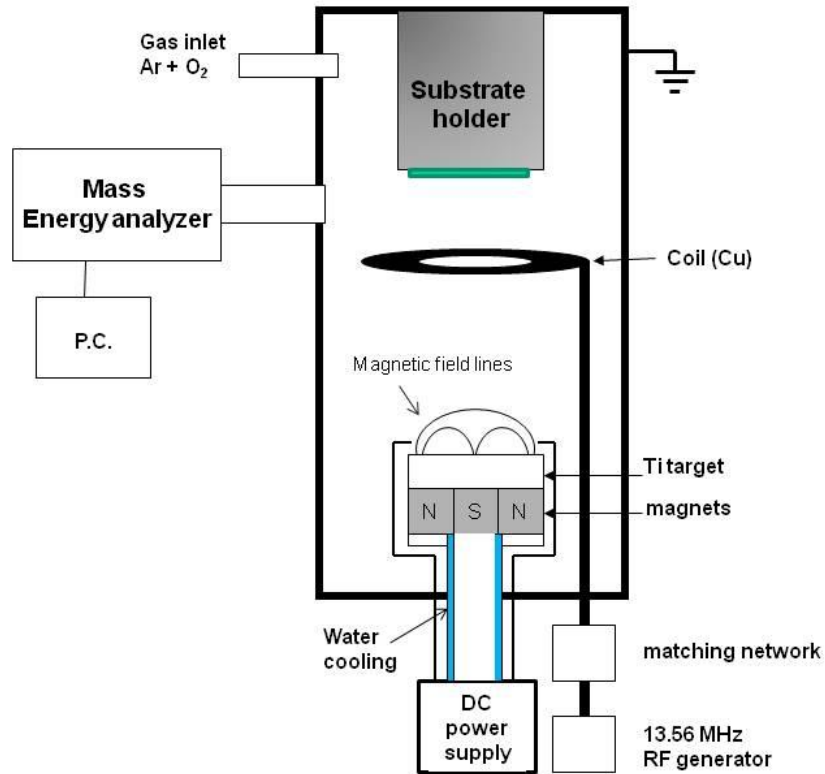


Fig. 1.

Schematic representation of the vacuum chamber (VC1 and VC2) used for the IPVD deposition experiments. The DC power supply can be substituted by a pulsed power supply in order to generate high-power pulses on the magnetron target. The copper coil can be removed too. Here, only the mass spectrometer is shown but all the other diagnostic experiments (OES, AAS, LP) were performed in the same plane, at the same distance from the magnetron target.

Fig. 2:

Evolution of the average electron energy and the electron density (as deduced from the integration of the EEDF) and measured 2 cm above the induction coil as the RF power supplied to the coil is increased for a magnetron power of 100 W. The argon pressure was set either to 5 mTorr (Fig 2a) or to 30 mTorr (Fig 2b).

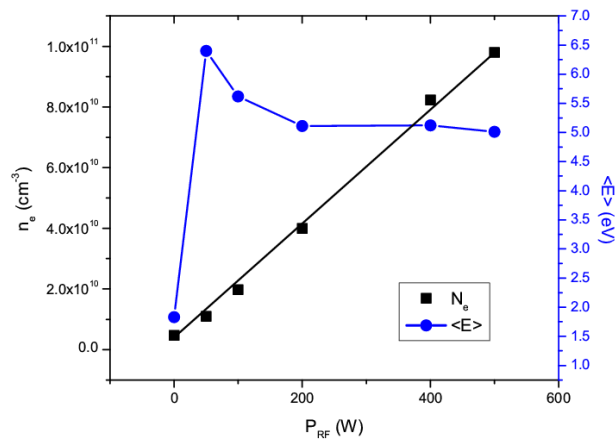
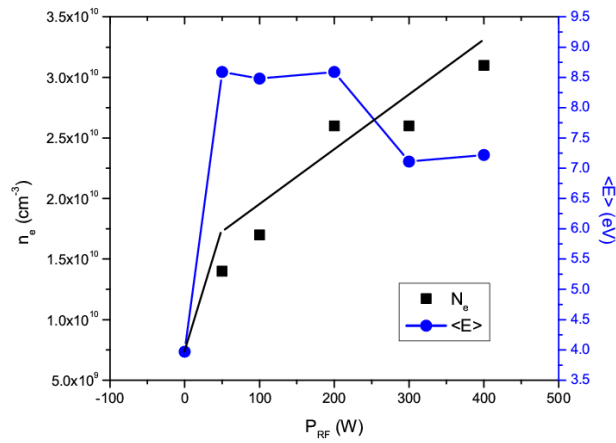


Fig. 3: Time – resolved optical emission spectroscopy data of the HiPIMS discharge in the poisoned mode, with 50% of oxygen at 1 Pa.

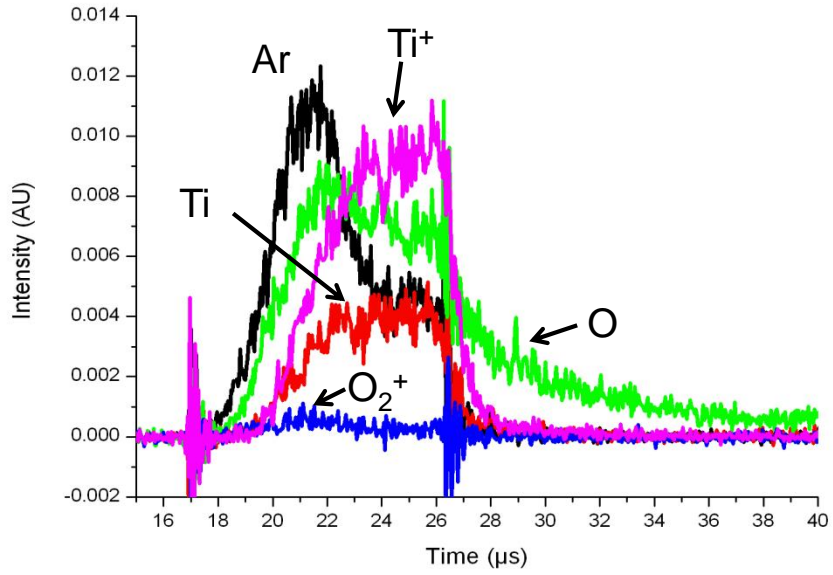


Fig. 4. Time-averaged mass spectrum of the HiPIMS discharge run in the oxidized regime.

